applied sciences

MDPI

Article

Base Isolation Compared to Capacity Design for Long Corner Periods and Pulse-Type Seismic Records

Dietlinde Köber [1,*], Felix Weber [2], Eugen Lozincă [1] and Viorel Popa [1]

1 Reinforced Concrete Department, Technical University of Civil Engineering Bucharest, Bucharest 020396, Romania
2 Maurer Switzerland GmbH, 8118 Pfaffhausen, Switzerland
* Correspondence: dietlinde.kober@utcb.ro; Tel.: +4021-2421208

Featured Application: Practical engineers should gain confidence in base isolation as an alternative to stiffening, a possible design approach for new as well as for existing buildings even under rare seismic conditions (in large corner period areas and for pulse-type seismic records). This article presents the structural benefits of curved surface sliders on a specific, existing building application. Moreover, authorities should be encouraged by the information included in this article, to emphasize alternatives to the stiffening design approach even under such special seismic conditions.

Abstract: Southern Romania is a geographic region with alluvial deposits. This soil type leads to rather long corner periods and provides as a particularity of the response spectrum an enlarged plateau. These conditions produce large displacement demands. Moreover, pulse-type ground acceleration records make this seismic area more unique. Research on the seismic behaviour of structures built under such unusual conditions is limited and Romanian engineers are not confident to apply alternative solutions such as base isolation. Although capacity design is still the regular design method applied in Romania, modern base isolation solutions may overcome the large displacement demand expectation produced by seismic events and fulfil immediate occupancy requirements. This study presents the seismic performance of an existing hospital from Bucharest, for which two seismic design solutions were applied: (i) classical approach based on capacity design and (ii) base isolation. Both approaches are compared in terms of drift, acceleration and base shear values. Static as well as non-linear dynamic analysis methods were applied.

Keywords: seismic behaviour; hospital building; non-linear dynamic analysis; push-over analysis; curved surface sliders

check for updates

Citation: Köber, D.; Weber, F.; Lozincă, E.; Popa, V. Base Isolation Compared to Capacity Design for Long Corner Periods and Pulse-Type Seismic Records. *Appl. Sci.* **2023**, *13*, 1217. https://doi.org/10.3390/app13021217

Academic Editors: Jong Wan Hu and Junwon Seo

Received: 9 November 2022
Revised: 3 January 2023
Accepted: 6 January 2023
Published: 16 January 2023

1. Introduction

The paper addresses the effectiveness of base isolation in long corner period areas under pulse-type seismic records, (see Section 2). Southern Romania experiences intermediate-depth earthquakes (depths between 60 and 200 km) with low frequency content, seismic conditions that brought severe damage or collapse to a wide range of flexible buildings during past earthquakes. Similar frequency content is typical for the Mexico City area, but there it is coupled with bright-band seismic records [1]. Under these rather unique seismic conditions, the confidence of local practical engineers in base isolation effectiveness is rather low. Currently, Romania counts only four base-isolated buildings: the Victor Slavescu Building of the Management Studies Academy, the City Hall, and the Arc de Triomphe, all in Bucharest, and the INFLPR building in Magurele. Worldwide, the issue of base-isolated structures in near-fault areas (although for corner period values T_c of up to 1.0 s) has been addressed; for example in California, at the Loma Linda Medical Center [2] and Christchurch Women's Hospital [3]. Moreover, recent studies underline the importance of near-fault ground motions to the seismic response of the ground [4,5]. The authors have chosen an existing hospital building in Bucharest (corner period Tc = 1.6 s, of irregular plan and elevation, for which construction drawings were available (see Section 2). Advantages and the structural impact of base isolation are outlined.

Base isolation of buildings is considered worldwide a suitable alternative to the classical design approach based on the capacity method [6–8]. Due to decoupling of the super-structure from the foundation ground, the earthquake input for the isolated building was reduced dramatically. In this way not only structural elements, but especially the building content (non-structural elements, equipment, furniture) are protected from damage. Currently, an increasing number of people choose base isolation for the seismic protection of their homes. For example, in 2017 in Japan, approximately 4300 commercial and multi-family residential buildings, and more than 5600 single family homes were provided with base isolation systems [7].

Hospital buildings especially, should remain operational after important seismic events, in order to shelter and help injured people [9]. Immediate occupancy requirements can be fulfilled through an elastic seismic response. Two possible seismic design solutions are compared: (1) a stiffening approach—expecting high response acceleration and damage [10–13] and (2) base isolation [14–16].

Despite the advantages that base isolation offers (reduced damage expectation, functionality after important seismic events), its efficiency is still questionable in high corner period regions, which request high displacement demands [1,17]. Therefore, the authors conducted a study on an existing hospital building from Bucharest, the capital city of Romania (which is a high corner period region, Tc = 1.6 s [18–22].

Two design approaches, a classical stiffening solution and a base isolation design were analytically compared. Modal analysis (for design) and static as well as non-linear dynamic analysis (for checking the structural behaviour) were performed [23–25]. Ambient vibration measurements helped estimating the building's modal periods [26]. Further experimental investigations, for example for the validation of analytical results, were not possible, especially due to the large dimensions of the analysed structure.

Due to their special characteristics (reduced sliding path due to double curvature and enlarged damping by properties of sliding surface) Curved Surface Sliders were chosen for the base isolation solution [9,27,28]. Other slider types (like High Damping Rubber Bearings or Lead-Plug Rubber Bearings) were not investigated due especially to their larger sizes, which significantly increases the cost of the base isolation solution.

2. Materials and Methods

2.1. Hospital Building

The analysed RC frame structure is part of a public hospital in Bucharest. The building has plan layout dimensions of approximately 12 $\times$ 28 m and an aboveground height equal to 16.55 m. The building has one underground and five above ground storeys. The storey heights range between 3.20 m and 3.50 m. A 30% area setback is present at the first two levels (see red area in Figure 1a), generating in-plane and elevation irregularity [18].

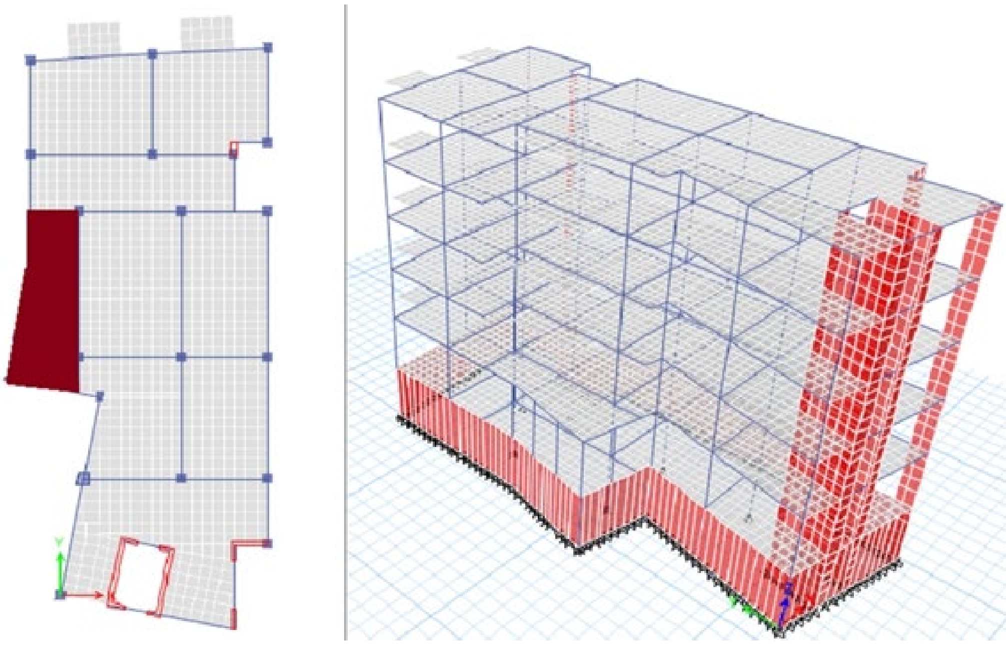

(**a**) (**b**)

Figure 1. ETABS structural model [29,30]: (**a**) ground floor plan layout; (**b**) 3D-view.

Plan irregularity is generated also by the positioning of the vertical circulation wall assembly. Displacements along the structural perimeter for an earthquake in X-direction are amplified by 37% compared to the mean floor displacement. Details regarding the influence of irregularity on the structural seismic response have been explained in [30].

The hospital building was originally designed according to the capacity spectrum method based on the provisions of P100-1/2006, [19]. The project was completed in 2012. Limited research on the seismic behaviour of base-isolation buildings located in long predominant period seismic regions for pulse-type accelerograms has been performed so far [1]. To increase the confidence of structural engineers in the base isolation system as an alternative to the classical structural solutions, under special seismic conditions, the current study has been planned. Bucharest was chosen for this study as it is situated in the southern part of Romania, in a seismic area with corner period Tc = 1.6 s. Pulse-type accelerogram recordings were obtained in Bucharest. In this attempt, the base-isolated building was designed considering the original building layout. The dimensions of the main structural elements are shown in Table 1 for both design approaches.

Table 1. Current structural element dimensions (cm).

Element	Classic Design	Design with Base Isolation
beams (bw × hw)	40 × 50, 40 × 60	25 × 50, 25 × 60
columns (bc × hc)	60 × 60	50 × 50
walls' thickness (bw)	20	20
slabs' thickness (hsl)	15	15

A 60 cm thick foundation mat was considered for both models. The isolation level was placed beneath the underground level. Isolators are supported by the mat foundation and connected to a foundation beam girder, which supports the entire structure. This solution turned out to be more economic than a double raft foundation, although it preserves less usable area.

The structural analysis for the design of both structural solutions was performed using the ETABS software 2013 [29]. The capacity spectrum method was used for structural analysis. Once designed, the seismic performance of the structures was investigated in the non-linear range of behaviour by using the PERFORM 3D software 2006 [31]. Non-linear static analysis and non-linear time history analysis were performed. A 3D view of the PERFORM 3D software structural model is shown in Figure 2. While EATBS gives the opportunity of a more refined structural model, PERFORM 3D brings the benefits of fast non-linear dynamic computation.

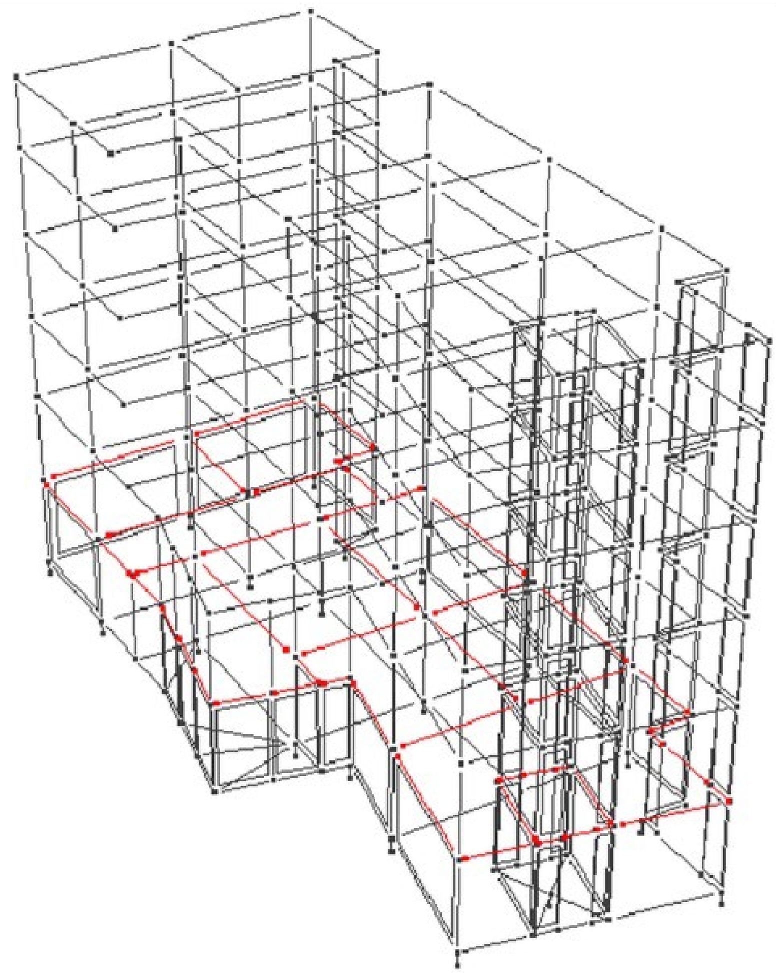

Figure 2. 3D structural view [31].

The computed base shear, lateral displacement and horizontal accelerations were compared for both design approaches. Double curved sliding isolators produced a structural design optimization by isolator dimensions reduction. Isolators were designed for a chosen isolation period (4.4 s) in order to obtain a minimum response spectrum ordinate. According to [16] the design earthquake for the Ultimate Limit State has a 225 year return period (20% probability of exceedance in 50 years). The spectrum compatible records considered in this study comply to the design spectrum. A 475 years return period (10% probability of exceedance in 50 years) was considered as maximum expected earthquake [32]. Isolators were designed to reach 64.2 cm displacement capacity.

2.2. Seismic Input for the Bucharest Region

The Vrancea earthquake source affects most of the Romanian territory, including Bucharest. It produces intermediate depth seismic events with low frequency content. Long predominant period values (of up to Tc = 1.6 s) are typical for the southern part of Romania (Figure 3a). Peak design ground acceleration values of up to 0.4 g for the 225 year mean return period earthquake are expected (Figure 3b).

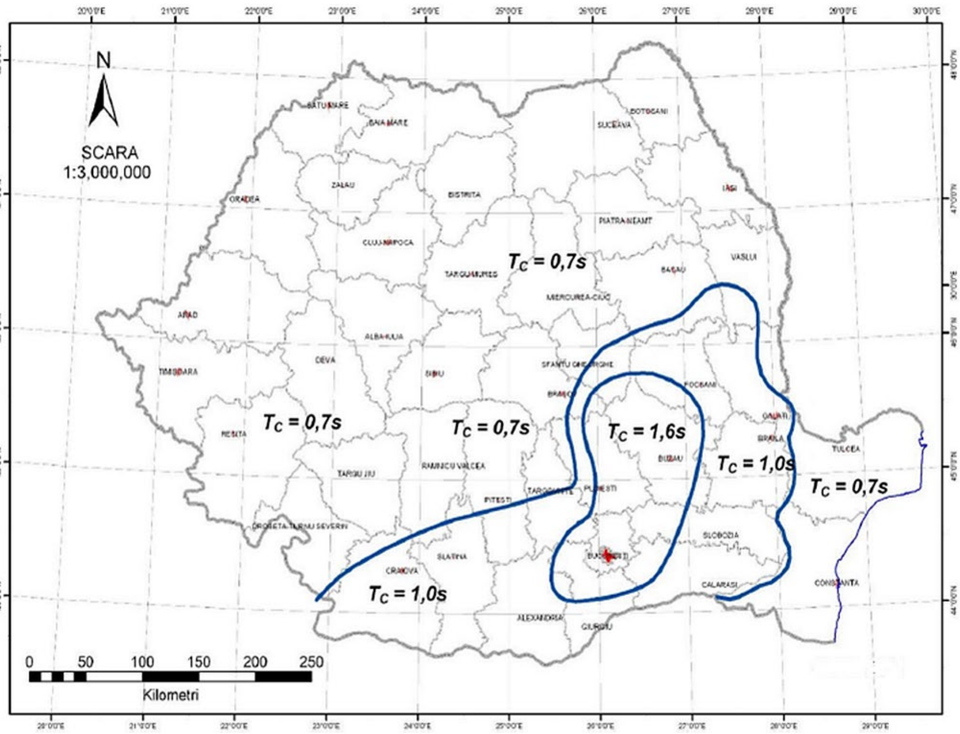

(a)

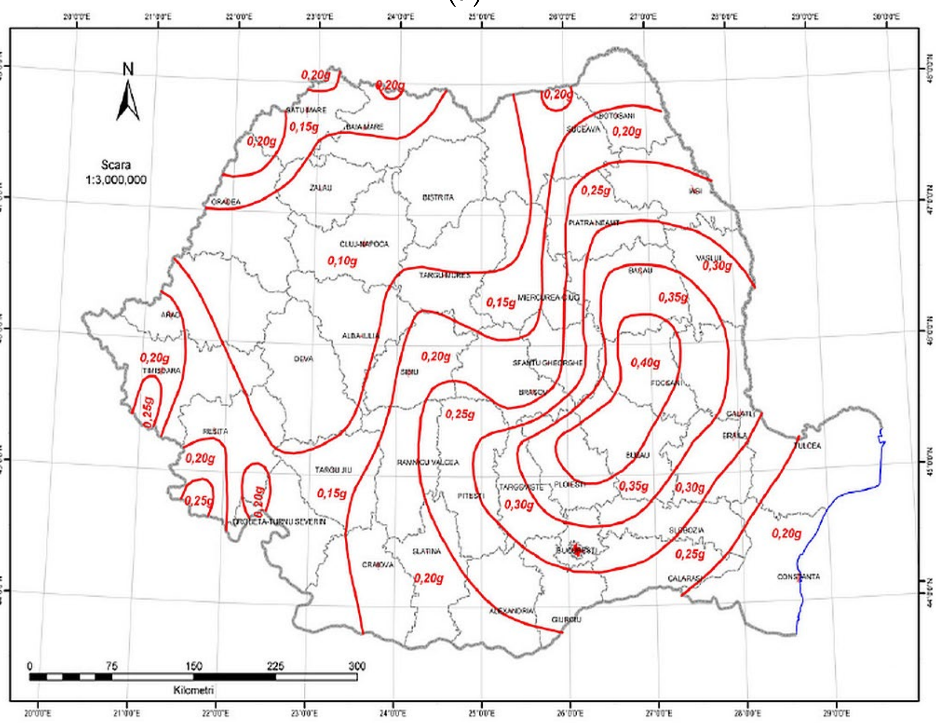

(b)

Figure 3. Seismic area information for Romania [18]: (**a**) corner period values, Tc distribution; (**b**) design ground acceleration values for earthquakes with return period of 225 years.

Long predominant period values, high design ground accelerations and pulse-type ground acceleration records typical for strong Vrancea seismic events (Figure 4) join, making the southern part of Romania a rather unique seismic area [1]. Such earthquakes concentrate more than 90% (Figure 4d) of their energy in only one pulse.

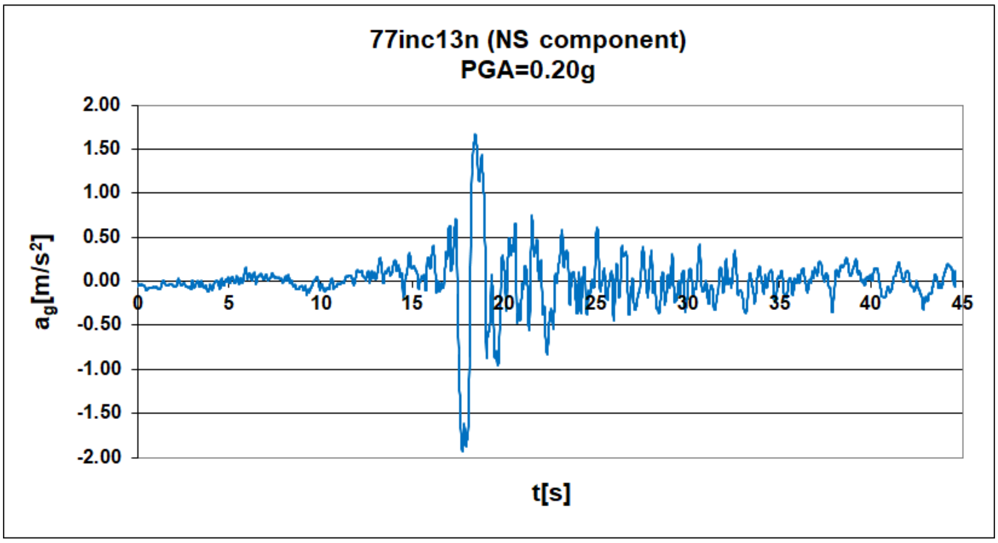

(**a**)

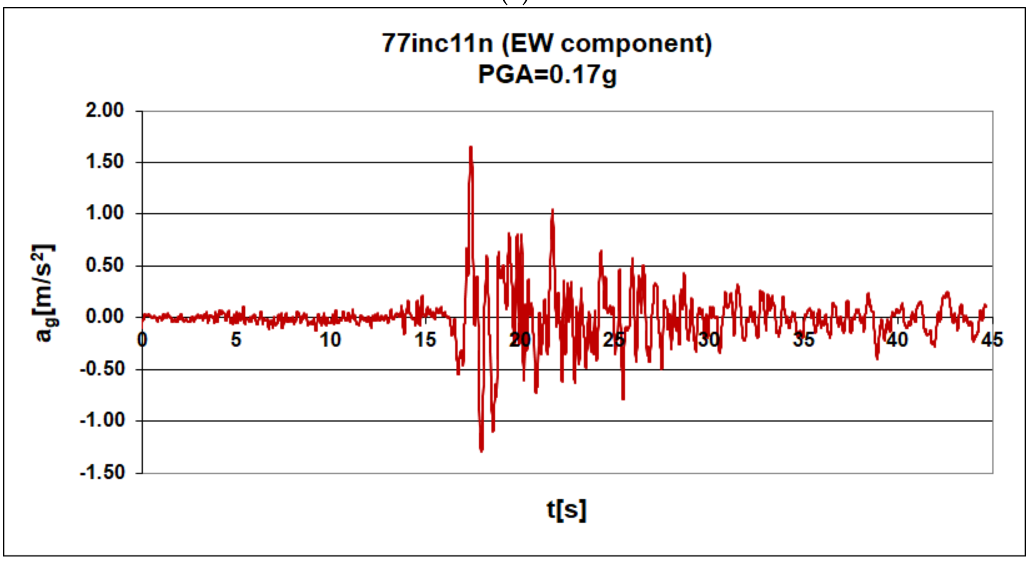

(**b**)

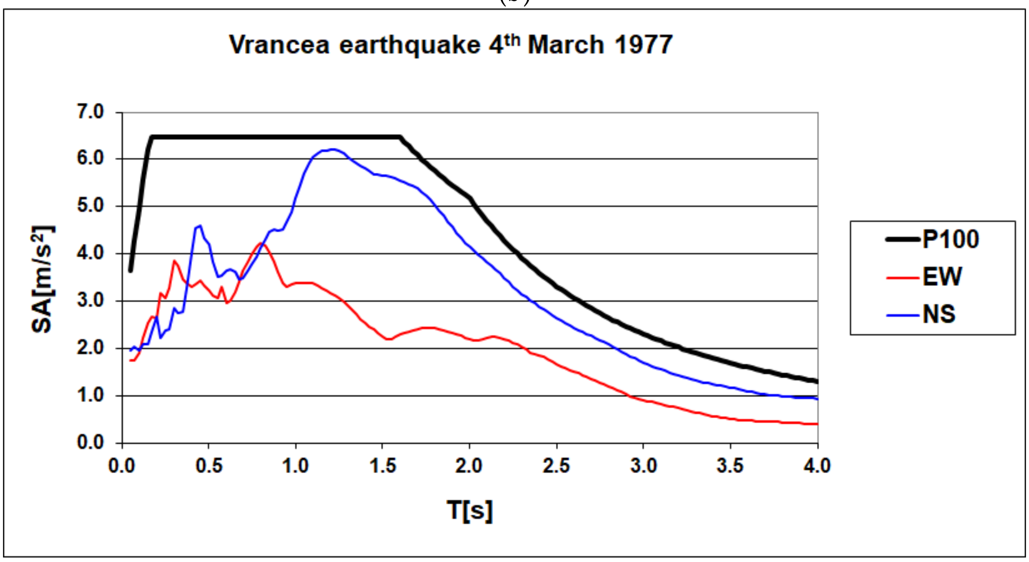

(**c**)

Figure 4. *Cont.*

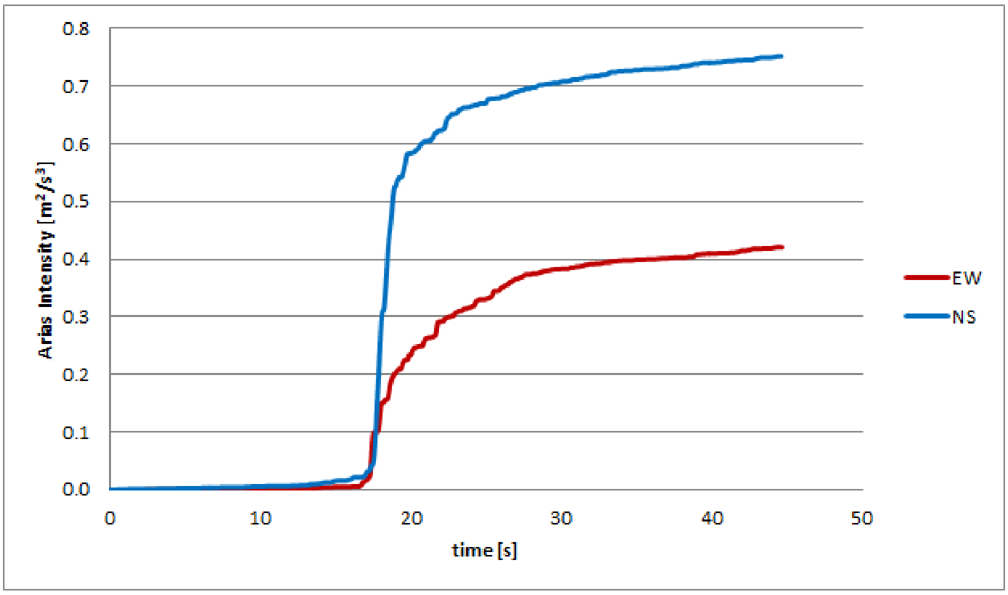

(**d**)

Figure 4. Vrancea earthquake of 4 March 1977 (M = 7,4 Richter Scale), INCERC monitoring station: (**a**) horizontal acceleration record from the NS direction; (**b**) horizontal acceleration record from the EW direction; (**c**) absolute acceleration spectrum of Figure 4a,b records and from P100-the Romanian seismic design code [18]; (**d**)Arias intensity.

These special seismic input characteristics generate extremely high lateral displacement demands (over 45 cm in Bucharest and over 60 cm in areas with an expected design acceleration of 0.4 g), which buildings should withstand when a design earthquake occurs. If capacity design method is applied, the high lateral displacement demand directly influences the strength and ductility of the structural elements.

There is a limited experience worldwide with such highly predominant periods of the design ground motion and pulse type ground motion. For example, the long predominant period of ground motions in Mexico City produce bright-band acceleration records [33]. This means that the earthquake energy is distributed over a large frequency range and so the influence on the structural elements is diminished compared to a pulse-type accelerogram [1].

The horizontal acceleration record from the NS direction (Figure 4a) acts in the structural main X-direction and the horizontal acceleration record from the EW direction (Figure 4b) acts in the structural main Y-direction (Figure 1).

2.3. Finte Element Modelling

ETABS 2013 [29] was used for the design process while PERFORM 3D 2006 [31] was used for the structural performance check.

In the ETABS model (Figure 1), the beams and columns were modelled as frame elements and the slabs and walls as shell elements. Vertical loads were applied as uniform loads on slabs and linear distributed loads along the perimeter beams. Wind loads were neglected, due to their inferior influence on the structural behaviour, compared to the effect of horizontal earthquake loads.

In the PERFORM 3D model (Figure 2) frame elements with concentrated plastic hinges at their ends were used to model beams and columns. The behaviour of the plastic hinges was modelled using a trilinear bending moment–rotation relation. The rotation capacity of the plastic hinges was computed according to [34], considering the mean strength of concrete and steel. Walls were modelled as shell elements with fibre sections. Linear behaviour was considered for the shear response. In order to model the wall-beam connections, especially when beams are supported on a perpendicular wall, columns withas fibre sections were defined at wall ends. These columns model the axial behaviour of wall ends, whereas the contributing wall area assures the bending behaviour of the columns perpendicular to the wall. As an alternative for modelling columns at wall ends, frame elements having axial plastic hinges were considered, but convergence problems were encountered.

The stiffness of structural elements was reduced at 50% to account for the concrete cracking [18].

Details regarding the first six Eigen modes for the upper structure are presented in Table 2 (arrows show the translation direction).

Table 2. Eigen modes of over ground structure, ETABS software.

Mode Number	**1**	**2**	**3**	**4**	**5**	**6**
frequency [Hz]	1.75	2.03	2.30	5.56	7.04	8.06
mass ratio [%]	66% → translation	65% ↑ translation	15% → translation 51% torsion	9%→ translation 2% torsion	10%↑ translation 4% torsion	6% ↑ translation 7% torsion

2.4. Curved Surface Slider as Base Isolator

Given the particularities of Vrancea seismic source (see also Section 2.2) CSS-Curved Surface Sliders were chosen for the isolation system. The two most important advantages of these sliders are (1) the reduction of the isolator displacement (due to the double curvature) and (2) the high damping of the earthquake-induced movement (due to friction along the curved sliding surface). In this way, the isolator dimensions are reduced to a minimum and reduced dimensions of the isolator supporting structural elements (for example the underground columns) are achieved, making the solution more cost-efficient.

Base isolation devices need to be designed for the design earthquake (DBE) and their sliding capacity must be checked under maximum expected earthquake (MCE) conditions [35].

The Romanian Standard for seismic design [18] indicates for the seismic area of Bucharest a design earthquake with return period of 225 years and a maximum expected design ground acceleration of 0.3 g. The characteristics of the isolator devices designed for DBE are shown in Figure 5.

In Figures 5 and 6, the following terms are used: μ_{opt}—optimum friction, d_{bd}—isolator displacement, ζ_{eff}—effective damping, T_{eff}—effective isolation period, T_{iso}—isolation period, R_{eff}—isolator curvature radius, E_S—elastic energy reversibly stored in the isolation system, E_h—histeretic dissipated energy, k_{rest}—restoring stiffness force, N_S—gravity load on isolator.

In the PERFORM 3D software the sliding isolation devices were modelled considering the horizontal force–displacement relations, the restoring stiffness, the displacement capacity and the initial stiffness (until the friction is overrun). The restoring stiffness and displacement capacity result from the isolation device design. The initial stiffness was chosen 100 times larger than the restoring stiffness (to limit the initial displacement, until friction is overrun). As supplementary details, the following sliding isolation device characteristics were considered: the friction coefficient, the radius of the sliding surface and the stiffness for axial compression loads. An earthquake with return period of 475 years and maximum expected horizontal ground acceleration of 0.375 g was considered as the MCE event ([32,36]). The characteristics of the isolator devices designed for the MCE are shown in Figure 6.

Because of the building layout (closely spaced columns in some parts of the building) and in order to catch up with the elevator shaft, isolation devices were placed beneath the underground level, on a foundation mat. They directly support a foundation beam girder. This was designed to reduce material consumption for the foundation system.

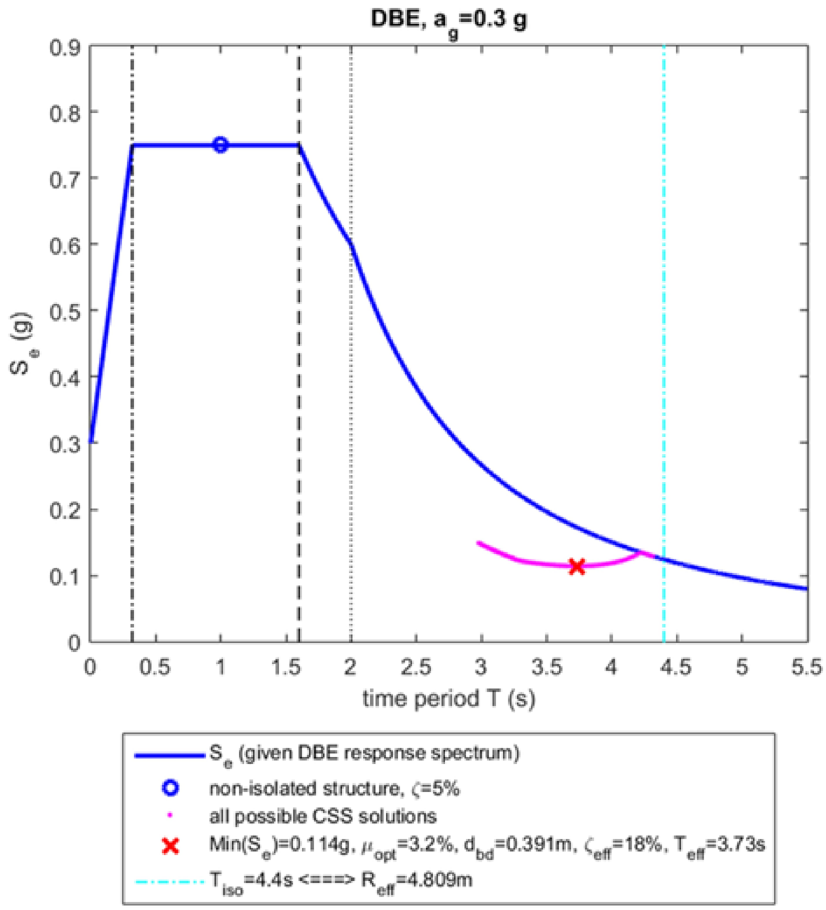

(**a**)

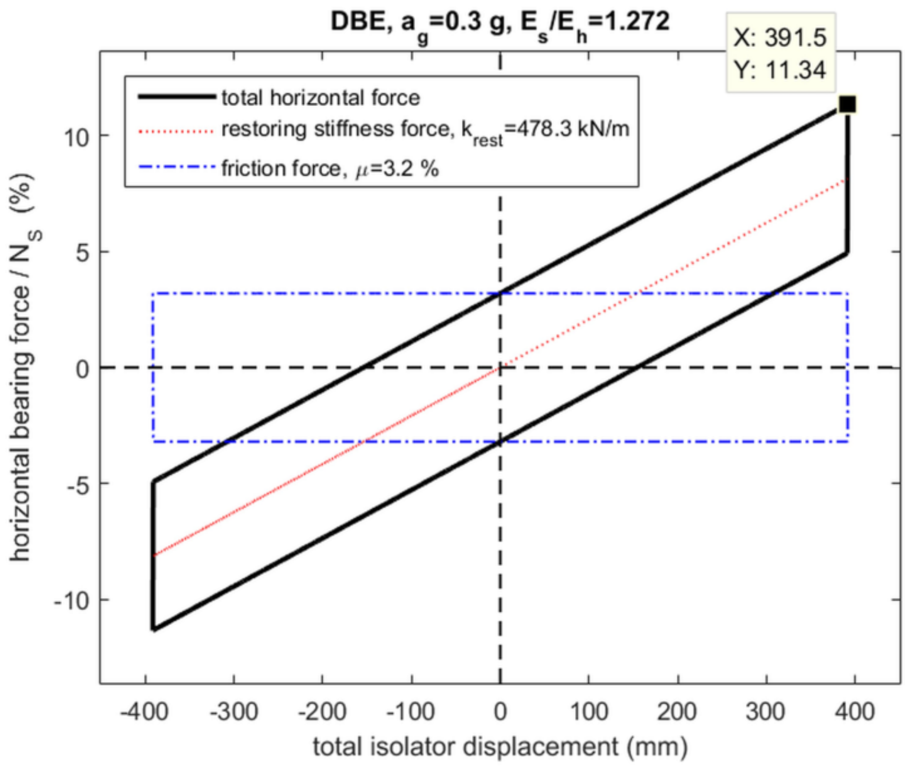

(**b**)

Figure 5. Design CSS: (**a**) optimization; (**b**) displacement capacity.

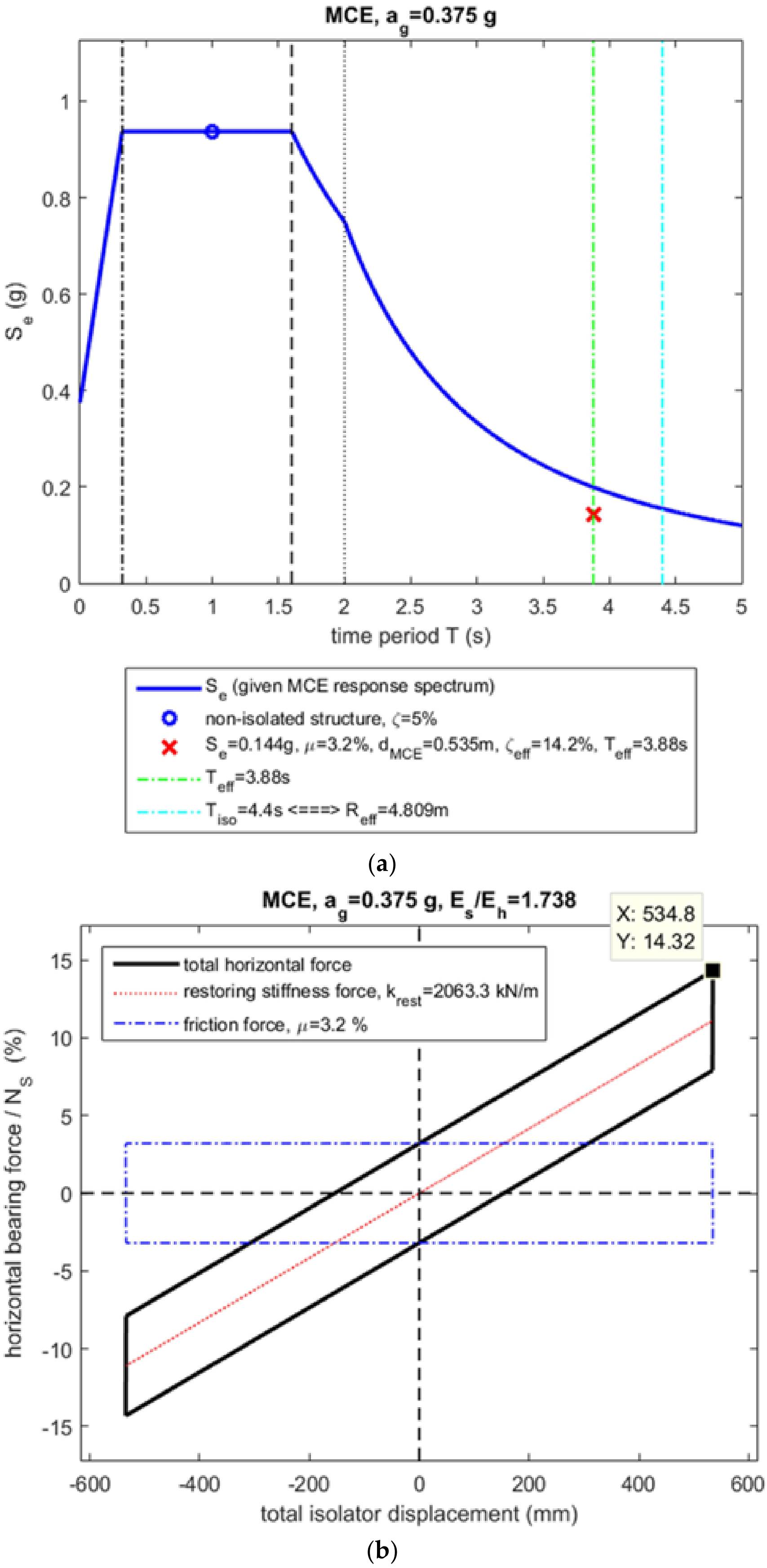

Figure 6. Behaviour CSS for MCE: (**a**) response spectrum; (**b**) displacement capacity.

Figure 7 shows indicative double curved surface slider dimensions for the analysed structure. Even in large corner period areas such as Bucharest, the double sliding path given by the upper and lower slider curvature provides feasible slider dimensions.

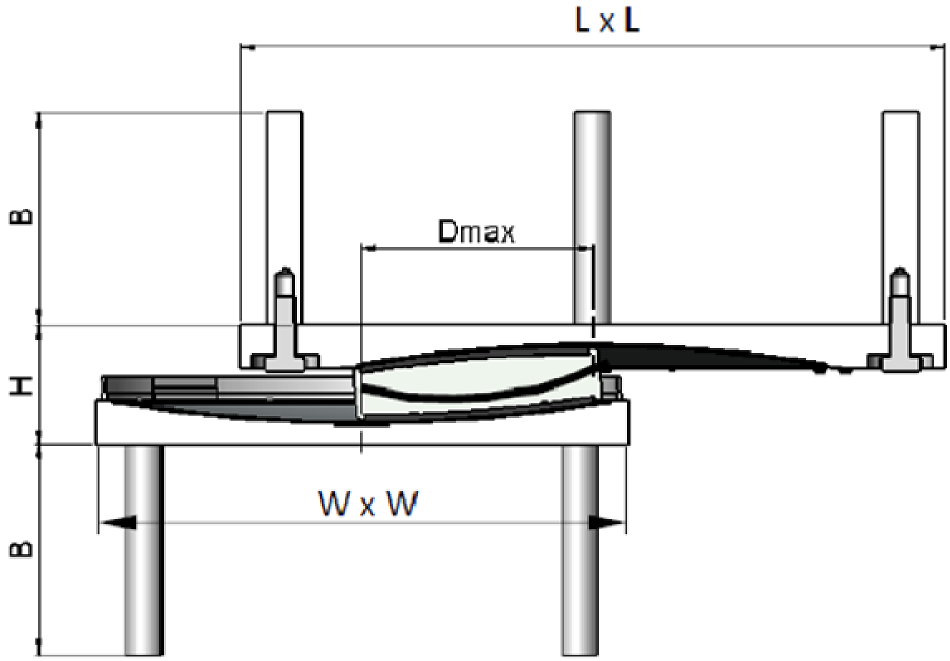

Figure 7. Indicative slider dimensions: L = 1,53 m; W = 1,08 m; B = 0,3 m; H = 0,17 m; D_{max} = 0,6 m [37].

3. Results

3.1. Structural Performance during Design Earthquake

Structural analysis was performed using the PERFORM 3D software in order to check the structural behaviour by:

- non-linear static (push-over) analysis—to evaluate the structural strength and deformation capacity;
- non-linear time-history analyses—to determine the structural behaviour subjected to ground motions.

For the non-linear time-history analyses, three natural accelerograms (INCERC Bucharest station seismic records from the Vrancea earthquakes of 1977, 1986 and 1991) and three spectrum-compatible accelerograms (considering the design spectrum of [18] for corner period Tc = 1.6 s) were selected. Seismic action combination rules given in [18,32] (100% along one and 30% in the other main direction) were used. The vertical earthquake component was applied as well. The results are presented hereinafter for the weakest main structural direction (X-direction or small plan layout dimension).

3.1.1. Building Design According to the Capacity Method

The force–displacement relation (total earthquake force at the bottom of the upper structure and horizontal displacement in the centre of mass at the upper level) is shown in Figure 7 and results are detailed in Table 3.

The displacement demand of 40 cm was determined according to Annex B of EN 1998-1 [32]. The model was pushed in the horizontal direction up to a displacement equal to 1.5 the displacement demand.

The overall strength of the building designed according to the capacity method is equal to 3. The ratio between horizontal failure force and building weight equals 5861/18,972 = 0.3. This is three times the global seismic coefficient considered for design.

Table 3. Details regarding the force–displacement curve shown in Figure 8.

Stage	Horizontal Force [kN]	Displacement [m]	Remarks
yield	3655≈ 1.97 design force *	0.041	-
first failure	4883≈ 2.7 design force *	0.079	30% of beam plastic hinges have failed
total failure	5861≈ 3.2 design force *	0.163	90% of beam plastic hinges have failed; 25% of ground floor columns have failed

* design force represents the horizontal earthquake force considered for structural design.

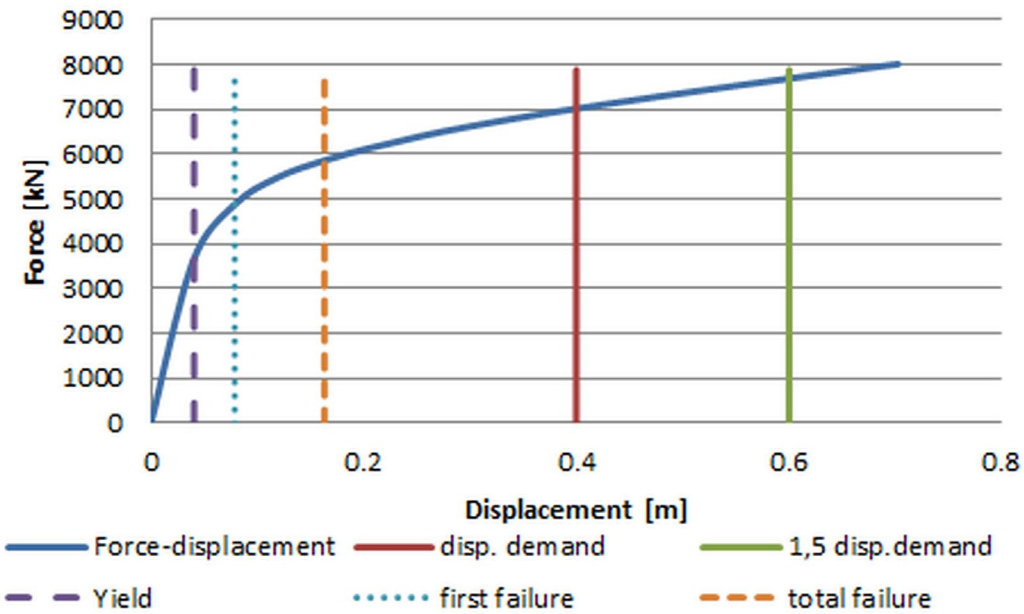

Figure 8. Force–displacement curve for the capacity design of the building, X-direction.

The behaviour factor considered for the design was based on an α_u/α_1 ratio equal to 1.35 [18]. According to the force–displacement relation determined by non-linear static analysis, this ratio equals 0.163/0.041 ≈ 4.0. This is 2.9 times more the value considered in the design.

Results of the non-linear time history analysis are shown in Table 4 for the building designed according to the capacity method. For the results obtained using the three spectrum-compatible accelerograms, the mean values are presented.

Table 4. Results from non-linear time-history analysis for the building designed according to the capacity method.

Result	INCERC 1977 Original	INCERC 1986 Original	INCERC 1991 Original	Spectrum Compatible Tc = 1.6 s
Maximum base shear force [kN]	6108	3256	1260	7840
Maximum interstorey drift [‰]	7.40 OG1 *	2.80 OG1 *	0.86 OG2 *	12.10 OG2 *
Maximum acceleration at the underground level [g]	0.20	0.10	0.08	0.36
Maximum acceleration at the building top [g]	0.38	0.23	0.11	0.50

* OG represents over ground level.

3.1.2. Base-Isolated Building

For the baseisolated structure, the results of the non-linear time-history analyses are shown in Table 5. For the results obtained using the three spectrum-compatible accelerograms, the mean values are presented.

Table 5. Results from dynamic non-linear analysis, base-isolated building.

Result	INCERC 1977 Original	INCERC 1986 Original	INCERC 1991 Original	Spectrum Compatible Tc = 1.6 s
Maximum base shear force [kN]	1308	573	550	2068
Maximum interstorey drift [‰]	*	*	*	*
Maximum acceleration at the underground level [g]	0.19	0.10	0.091	0.26
Maximum acceleration at the building top [g]	0.21	0.06	0.079	0.27
Maximum isolator displacement [m]	0.21	0.007	0.005	0.32

* interstorey drift ratios smaller than 0.1%.

Using base isolation results in:

- a 45% drop in the maximum response acceleration at the top of the building;
- the isolation system accommodates up to 90% of the earthquake-induced horizontal movement. The structure above the isolation level moves like a rigid box. No yielding of structural elements is registered and no damage is foreseen;
- the base shear force is reduced by 65–80%.

The vertical earthquake component causes axial force variations of 4% in the range of high ground acceleration amplitudes. No axial tension forces were registered at the isolation layer.

3.2. Time Histories for Both Structural Approaches

Figure 9 shows absolute acceleration time histories in the mass centre for the INCERC 1977 spectrum-compatible accelerogram at the base of the structure (or quite over the isolation level for the base-isolated structure) and at the top of the building. The isolated structure manages most of the earthquake-induced movement at the isolation level and just 37% acceleration amplification is registered at the building top for the first strong pulse. As comparison for the building designed according to the capacity method, base horizontal accelerations are amplified by up to 84% at the building top.

Figure 10 shows the relative displacement time histories in the mass centre for the INCERC 1977 spectrum compatible accelerogram at the building's base (or quite over the isolation level for the base-isolated structure) and at the building top.

Relative displacements are amplified by up to 85% along the building height for the stiffened building, whereas for the base-isolated building negligible relative displacement differences are registered at the building top compared to the isolation level

The maximum relative displacement for the isolated building is delayed by 0.2 s at the building top with respect to the base of the building. The results for the stiffened building show the peak almost at the same time.

The base-isolated building experiences half of the top displacements registered for the stiffened building (see Figure 11a). Drift values are negligible for the base-isolated structure (Figure 11b).

Figure 12 shows the deformed shapes of the analysed structure, at maximum ground acceleration. The base-isolated structure experiences a rigid body movement while the fixed base structure presents a bending–shear deformation.

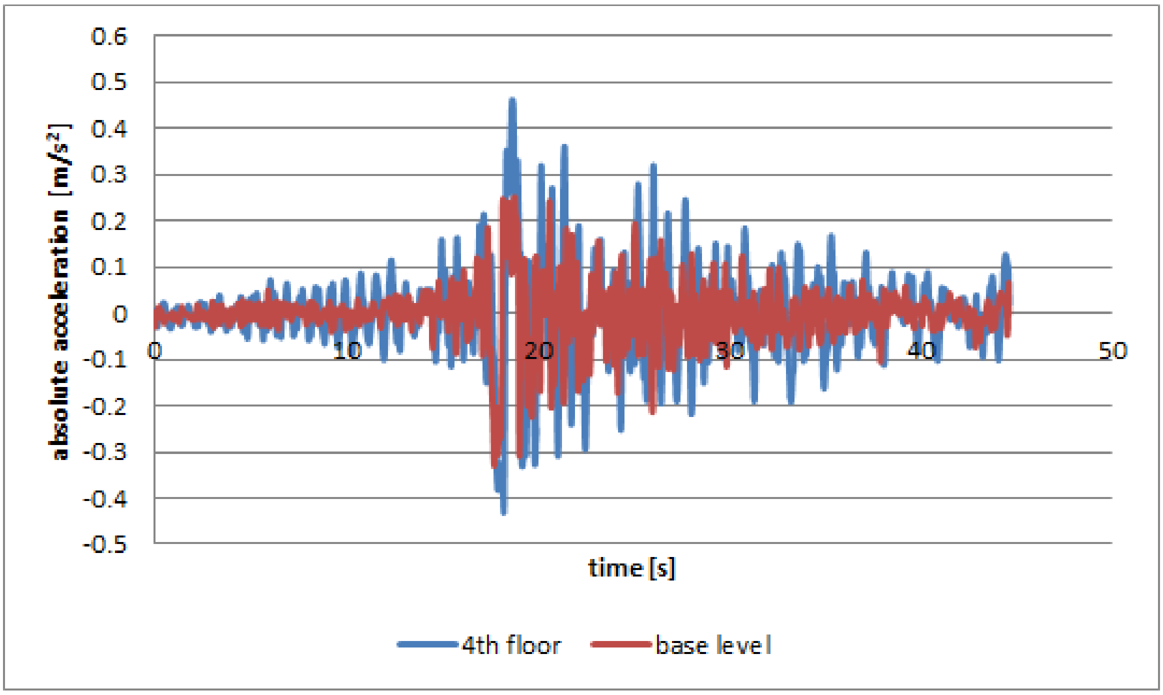

(a)

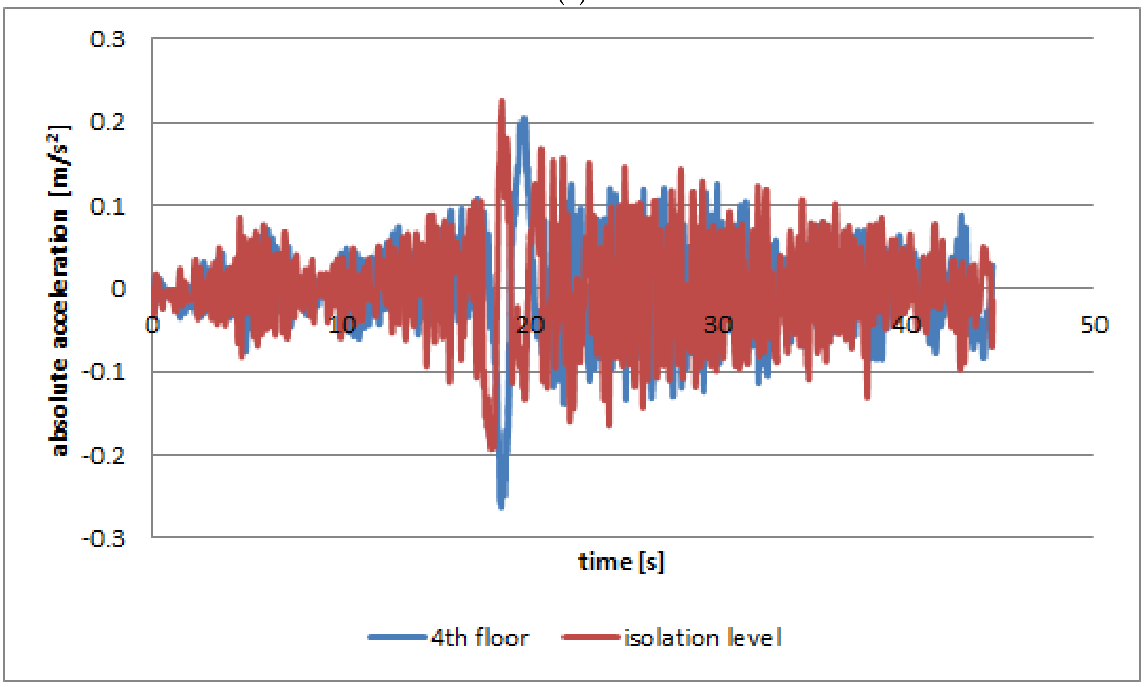

(b)

Figure 9. Absolute acceleration time histories, INCERC 1977 spectrum compatible ground acceleration record: (**a**) classic building; (**b**) base-isolated structure.

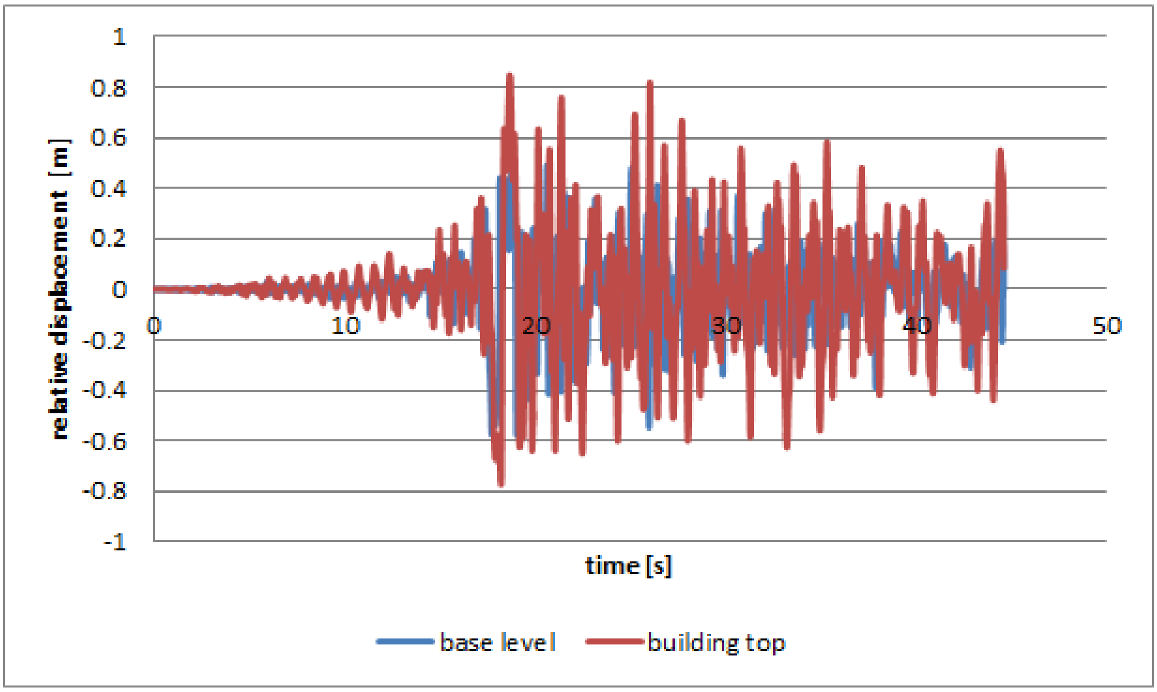

(**a**)

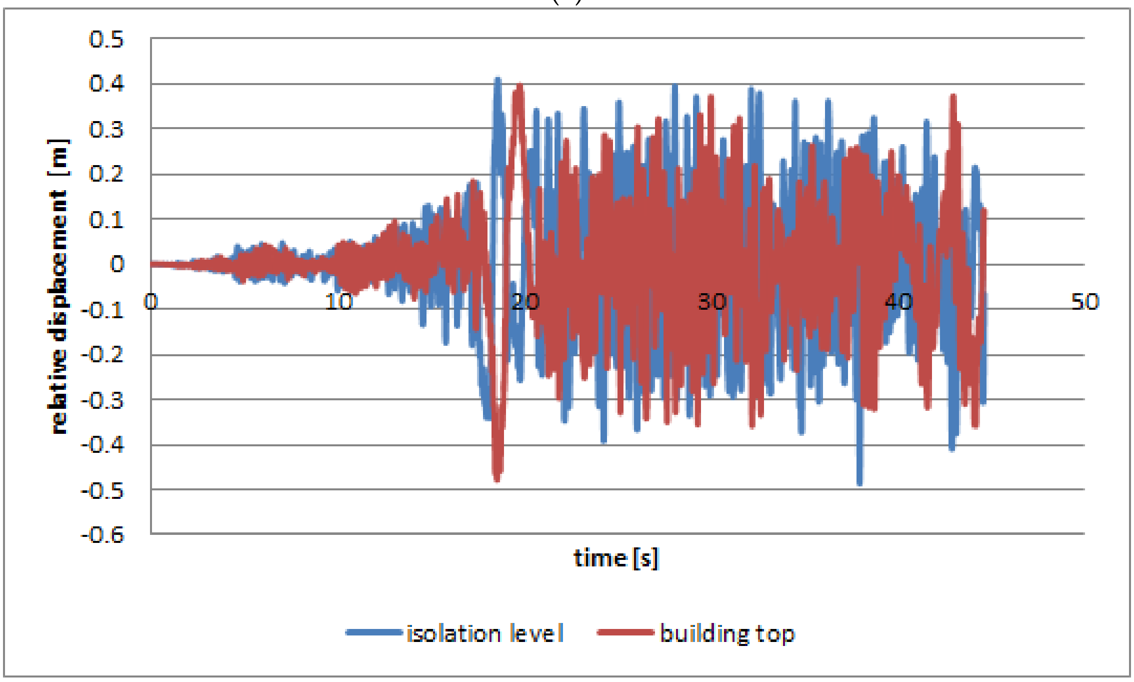

(**b**)

Figure 10. Relative displacement [m] time histories, INCERC 1977 spectrum compatible ground acceleration record: (**a**) classic building; (**b**) base-isolated structure.

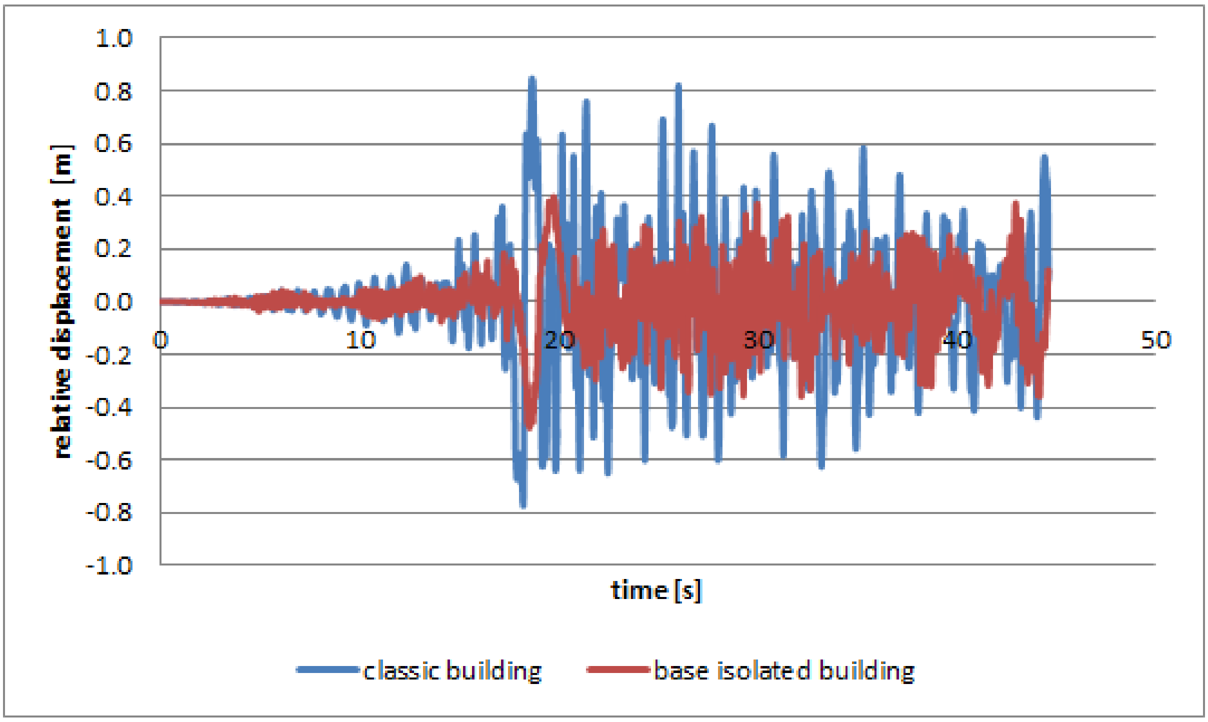

(a)

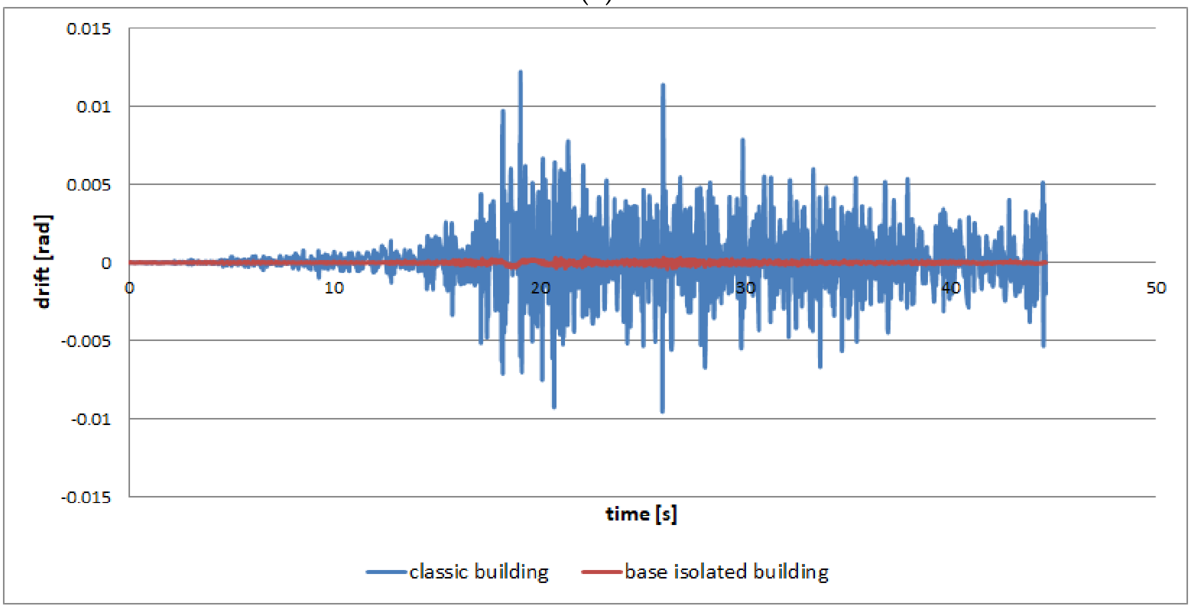

(b)

Figure 11. (**a**) Relative displacement [m] time histories at building top, INCERC 1977 spectrum compatible ground acceleration record; (**b**) drift time histories at level 1, INCERC 1977 spectrum compatible ground acceleration record.

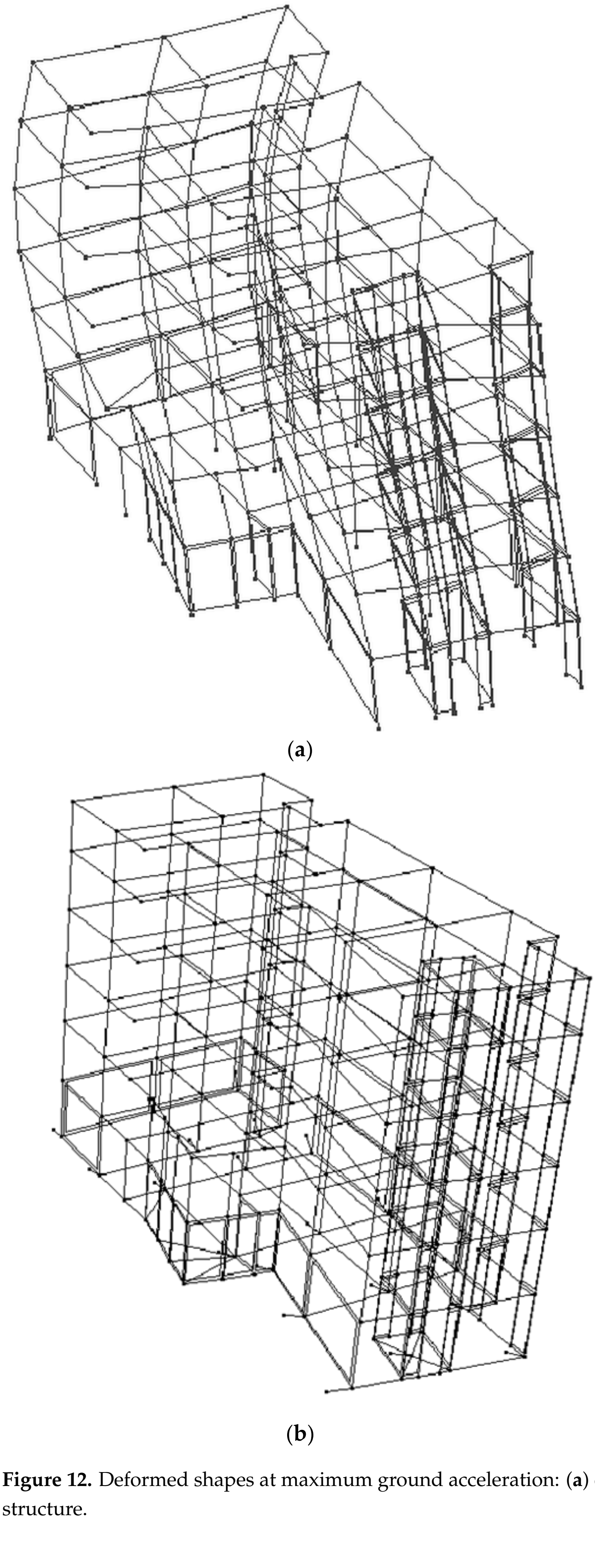

(**a**)

(**b**)

Figure 12. Deformed shapes at maximum ground acceleration: (**a**) classic building; (**b**) base-isolated structure.

4. Discussion

Base isolation is an effective structural solution in contrast to the "stiffening" design approach, even under special seismic conditions characterised by long predominant periods and pulse-type seismic ground acceleration records.

For the analysed building, a 45% drop of the floor acceleration at the top of the building was obtained by base isolation. This is likely to reduce the seismic damage of the acceleration sensitive components of the building. A total of 90% of the lateral displacement is concentrated in the isolation layer, protecting the upper structure from earthquake-induced damage in displacement sensitive components. A large reduction of the base shear force was observed as well.

Drift values for the isolated structure are negligible and plan irregularity effects are corrected by the isolation level. Detailed information upon the influence of plan and elevation irregularity on the seismic response of the analysed hospital building are shown in [30]. The stiffened structure experiences instead large drift values, expected to endanger the nonstructural components of the building.

The rigid body movement of the base-isolated structure is likely to inhibit any damage for the structural and nonstructural components of the building. This is of particular importance for the hospital buildings that are required to remain functional after the incidence of a strong earthquake.

Pulse-type seismic records may force isolators to reach their displacement capacity. In this study, the maximum displacement at isolation level was 0.49 m according to the performed time history analysis. This maximum displacement value is reached only during one pulse and it exceeds the DBE design isolator displacement capacity of 0.392 m. Nevertheless, isolators were checked to also withstand an MCE earthquake, according to which they have a displacement capacity of 0.535 m.

Curved sliders are sensitive to uplift for pulse-type seismic records. The analysed hospital building showed sufficient vertical loading such that the horizontal seismic action caused no uplift. All isolators remain functional even during the main shock.

Supplementary to the evident structural advantages encountered for the base-isolated solution of the analysed hospital structure, an economical comparison (as-built state as well as life-cycle analysis) is planned to be performed.

Author Contributions: Conceptualization, D.K. and F.W.; methodology, D.K.; software, D.K.; validation, E.L., V.P. and F.W.; formal analysis, D.K.; investigation, D.K. and F.W.; resources, D.K.; data curation, D.K.; writing—original draft preparation, D.K.; writing—review and editing, F.W., E.L. and V.P.; supervision, F.W.; project administration, D.K.; funding acquisition, D.K. All authors have read and agreed to the published version of the manuscript.

Funding: This research was funded by "Stiftung Maurer Söhne", Munich, Germany.

Institutional Review Board Statement: Not applicable.

Informed Consent Statement: Not applicable.

Data Availability Statement: Not applicable.

Acknowledgments: Framework and reinforcement drawings for the analysed structure were kindly provided by S.C. Consild S.R.L, Bucharest, Romania.

Conflicts of Interest: The authors declare no conflict of interest. The funder is represented by Felix Weber among the authors because he supported the study as follows: design of the curved slider isolators, technical data regarding the curved slider isolators, review of the manuscript.

References

1. Pavel, F.; Popa, V.; Văcăreanu, R. *Impact of Long-Period Ground Motions on Structural Design:A Case Study for Bucharest, Romania*; Springer: Berlin/Heidelberg, Germany, 2018; ISBN 978-3-319-73401-9.
2. Nielsen, G.; Rees, S.; Dong, B.; Chok, K.; Fatemi, E.; Zekioglu, A. Practical Implementation of ASCE-41 and NLRHA Procedures for the Design of the LLUMC Replacement Hospital. In Proceedings of the 2017 SEAOC Convention Proceedings. 2017. Available online: https://cdn.ymaws.com/www.seaoc.org/resource/resmgr/Convention_Proceedings/2017/030_PAPER_Nielsen.pdf (accessed on 3 November 2022).
3. Kuang, A.; Sridhar, A.; Garven, J.; Gutschmidt, S. Christchurch Women's Hospital: Performance Analysis of the Base-Isolation System during the Series of Canterbury Earthquakes 2011–2012. *J. Perform. Constr. Facil.* **2016**, *30*, 04015096. [CrossRef]
4. Zhu, C.; Cheng, H.; Bao, Y.; Chen, Z.; Huang, Y. Shaking table tests on the seismic response of slopes to near-fault ground motion. *Geomech. Eng.* **2022**, *29*, 133. [CrossRef]
5. Bao, Y.; Huang, Y.; Zhu, C. Effects of near-fault ground motions on dynamic response of slopes based on shaking table model tests. *Soil Dyn. Earthq. Eng.* **2021**, *149*, 106869. [CrossRef]
6. Lewis, S. The 10 largest Base-Isolated Buildings in the World. In ENR Engineering News-Record. 2017. Available online: https://www.enr.com/articles/42366-the-10-largest-base-isolated-buildings-in-the-world (accessed on 3 November 2022).
7. Mayes, R.; Aiken, I.; Taylor, A. *Revisiting Earthquake Lessons-Base Isolated Buildings*; Structural Engineers Association of California: Sacramento, CA, USA, 2019.
8. De Domenico, D.; Tubaldi, E.; Takewaki, I. Editorial: Recent Advances and Applications of Seismic Isolation and Energy Dissipation Devices. *Front. Built Environ.* **2020**, *6*, 126. [CrossRef]
9. Arranz, M.; Braun, C.; Huber, P. Seismic protection of the Eskisehir city hospital in Turkey. In *39th IABSE Symposium*; Engineering the Future: Vancouver, BC, Canada, 2017.
10. Moehle, J. *Seismic Design of Reinforced Concrete Buildings*; McGraw-Hill Education: New York, NY, USA, 2014; ISBN 978-0-07-183944-0.
11. Derecho, A.T.; Kianoush, M.R. Seismic Design of Reinforced Concrete Structures. In *The Seismic Design Handbook*; Naeim, F., Ed.; Springer: Boston, MA, USA, 2001. [CrossRef]
12. Fajfar, P. Analysis in Seismic Provisions for Buildings: Past, Present and Future. In *Recent Advances in Earthquake Engineering in Europe. ECEE 2018. Geotechnical, Geological and Earthquake Engineering*; Pitilakis, K., Ed.; Springer: Berlin/Heidelberg, Germany, 2018; Volume 46. [CrossRef]
13. Postelnicu, T.; Damian, I. *Proiectarea Structurilor de Beton Armat in Zone Seismice*; MarLink: Bucharest, Romania, 2012; ISBN 978-973-8411-83-8.
14. Mazza, F.; Mazza, M.; Vulcano, A. Base-isolation systems for the seismic retrofitting of r.c. framed buildings with soft-storey subjected to near-fault earthquakes. *Soil Dyn. Earthq. Eng.* **2018**, *109*, 209–221. [CrossRef]
15. Reddy, G.R.; Nagender, T.; Dubey, P.N. Seismic Base Isolation of Structures. In *Textbook of Seismic Design*; Reddy, G., Muruva, H., Verma, A., Eds.; Springer: Singapore, 2019. [CrossRef]
16. Sorace, S.; Terenzi, G. Analysis, Design and Construction of Base-Isolated Multiple Building Structure. *Adv. Civ. Eng.* **2014**, *2014*. [CrossRef]
17. Oliveto, N.D. Nonlinear Dynamic Analysis of Curved Surface Slider Systems under Harmoinc, Near-Fault and Long-Period Ground Motions. *J. Eng. Mech.* **2020**, *146*, 04020087.
18. *P100-1/2013*; Romanian Seismic Design Code Part I. Design Regulations for Buildings. MatrixRom: Bucharest, Romania, 2013.
19. *P100-1/2006*; Romanian Seismic Design Code Part I. Design Regulations for Buildings. MatrixRom: Bucharest, Romania, 2006.
20. Pavel, F.; Vacareanu, R.; Pitilakis, K.; Anastasiadis, A. Investigation on site-specific seismic response analysis for Bucharest. *Bull. Earthq. Eng.* **2020**, *18*, 1933–1953. [CrossRef]
21. Sokolov, V.; Wenzel, F.; Mohindra, R. Probabilistic seismic hazard assessment for Romania and sensitivity analysis: A case of joint consideration of intermediate-depth (Vrancea) and shallow (crustal) seismicity. *Soil Dyn. Earthq. Eng.* **2009**, *29*, 364–381. [CrossRef]
22. Grecu, B.; Zaharia, B.; Diaconescu, M. Characterization of site conditions for selected seismic stations in eastern part of Romania. *Acta Geophys.* **2018**, *66*, 153–165. [CrossRef]
23. Wilson, L.E. *Three Dimensional Static and Dynamic Analysis of Structures*; Computers and Structures Inc.: Berkeley, CA, USA, 2000; ISBN 0-923907-00-9.
24. Narasimhan, S.; Nagarajaiah, S.; Johnson, E.A.; Gavin, H.P. Smart base-isolated benchmark building. Part I: Problem definition. *Struct. Control. Health Monit.* **2006**, *13*, 573–588. [CrossRef]
25. Spacone, E.; Camata, G.; Faggella, M. Nonlinear models and nonlinear procedures for seismic analysis of reinforced concrete frame structures. In *Computational Structural Dynamics and Earthquake Engineering*; CRC Press: Boca Raton, FL, USA, 2007. [CrossRef]
26. Köber, D.; Aldea, A.; Enache, R.; Weber, F.; Semrau, P. Measured and computed dynamic characteristics of a hospital building in Bucharest. In Proceedings of the 5th International Conference on Smart Monitoring, Assessment and Rehabilitation of Civil Structures, Potsdam, Germany, 27–29 August 2019.
27. Saitta, F.; Clemente, P.; Buffarini, G.; Bongiovanni, G.; Salvatori, A.; Grossi, C. Base Isolation of Buildings with Curved Surface Sliders: Basic Design Criteria and Critical Issues. *Adv. Civ. Eng.* **2018**, *2018*. [CrossRef]

28. Weber, F.; Meier, L.; Distl, J.; Braun, C. Optimum design of curved surface sliders based on site-specific seismic input and its sensitivity. *Geosciences* **2018**, *8*, 83. [CrossRef]
29. CSI. *ETABS Integrated Building Design Software*; Computers and Structures: Berkeley, CA, USA, 2013.
30. Köber, D.; Semrau, P.; Weber, F. Design approach for an irregular hospital building in Bucharest. In *Seismic Behaviour and Design of Irregular and Complex Civil Structures IV*; Springer: Berlin/Heidelberg, Germany, 2022; ISSN 1573-6059.
31. CSI. Nonlinear analysis and performance assessment for 3D structures, version 4. In *CSI Perform-3D User Guide*; Computers and Structures: Berkeley, CA, USA, 2006.
32. *EN 1998-1/2004*; Design of Structures for Earthquake Resistance—Part 1: General Rules, Seismic Actions and Rules for Buildings. European Committee for Standardization: Brussels, Belgium, 2004.
33. Murillo, M.; Manuel, J. The 1985 Mexico Earthquake (PDF). In *Geofisica Colombiana*; Universidad Nacional de Colombia, Academia Colombiana de Ciencias Geofisicas-ACCG: Santafe de Bogota, Colombia, 1995; Volume 3, pp. 5–19, ISSN 0121-2974.
34. *EN 1998-3:2005*; Design of Structures for Earthquake Resistance. Assessment and Retrofitting of Buildings. European Committee for Standardization: Brussels, Belgium, 2005; pp. 35–42.
35. *EN 15129:2010-06*; Anti-Seismic Devices. DIN Deutsches Institut für Normung: Berlin, Germany, 2011.
36. *P100-3/2019*; Romanian Seismic Design Code Part III. Regulations for Seismic Evaluation of Existing Buildings. MatrixRom: Bucharest, Romania, 2019.
37. Maurer, S.E. Technical Specifications for Double Curved Surface Sliders. Available online: https://maurer.eu (accessed on 3 November 2022).